© 2014. Published by The Company of Biologists Ltd | Journal of Cell Science (2014) 127, 5253–5260 doi:10.1242/jcs.156554

RESEARCH ARTICLE

PTEN counteracts PIP_3 upregulation in spines during NMDA-receptor-dependent long-term depression

Kristin L. Arendt[1,*,§], Marion Benoist[2,‡,§], Argentina Lario[2], Jonathan E. Draffin[2], María Muñoz[2] and José A. Esteban[2,¶]

ABSTRACT

Phosphoinositide 3-kinase (PI3K) and PTEN have been shown to participate in synaptic plasticity during long-term potentiation (LTP) and long-term depression (LTD), respectively. Nevertheless, the dynamics of phosphatidylinositol-(3,4,5)-trisphosphate (PIP_3) and the regulation of its synthesis and degradation at synaptic compartments is far from clear. Here, we have used fluorescence resonance energy transfer (FRET) imaging to monitor changes in PIP_3 levels in dendritic spines from CA1 hippocampal neurons under basal conditions and upon induction of NMDA receptor (NMDAR)-dependent LTD and LTP. We found that PIP_3 undergoes constant turnover in dendritic spines. Contrary to expectations, both LTD and LTP induction trigger an increase in PIP_3 synthesis, which requires NMDARs and PI3K activity. Using biochemical methods, the upregulation of PIP_3 levels during LTP was estimated to be twofold. However, in the case of LTD, PTEN activity counteracts the increase in PIP_3 synthesis, resulting in no net change in PIP_3 levels. Therefore, both LTP and LTD signaling converge towards PIP_3 upregulation, but PTEN acts as an LTD-selective switch that determines the outcome of PIP_3 accumulation.

KEY WORDS: FRET, Hippocampus, PI3K, PTEN, Synaptic plasticity

INTRODUCTION

Phosphoinositides (phosphorylated derivatives of phosphatidylinositol) are asymmetrically distributed throughout intracellular compartments and the plasma membrane and, in this fashion, are thought to provide essential spatial and temporal cues for protein recruitment and intracellular membrane trafficking (Carlton and Cullen, 2005; Czech, 2003; Di Paolo and De Camilli, 2006; Downes et al., 2005). In neurons, the functional role of phosphoinositide metabolism and compartmentalization has been studied in great detail at the presynaptic terminal, where phosphoinositide turnover has been shown to be crucial for neurotransmitter vesicle cycling and synaptic function (Wenk and De Camilli, 2004).

[1]Department of Pharmacology, University of Michigan Medical School, Ann Arbor, Michigan 48109, USA. [2]Centro de Biología Molecular "Severo Ochoa", Consejo Superior de Investigaciones Científicas (CSIC)/Universidad Autónoma de Madrid (UAM), Madrid 28049, Spain.
*Present address: University of Stanford School of Medicine, Stanford, California 94305, USA. ‡Present address: INMED, INSERM, Aix-Marseille Université, Unité Mixte de Recherche 901, 13009 Marseille, France.
§These authors contributed equally to this work

¶Author for correspondence (jaesteban@cbm.csic.es)

Received 14 May 2014; Accepted 8 October 2014

Phosphatidylinositol-(3,4,5)-trisphosphate (PIP_3) is among the most elusive phosphoinositides. Basal levels of PIP_3 are extremely low, owing to a tight spatial and temporal regulation of PIP_3 synthesis (Vanhaesebroeck et al., 2001). Nevertheless, PIP_3 is enriched in specific subcellular compartments, such as the tip of growing neurites (Aoki et al., 2005; Ménager et al., 2004) and thin protrusions from dendritic spines known as spinules (Ueda and Hayashi, 2013). The synthesis of PIP_3 by phosphatidylinositol 3-kinases (PI3Ks) at the postsynaptic terminal is necessary for sustaining synaptic function, possibly by maintaining AMPA receptors (AMPARs) at the postsynaptic membrane (Arendt et al., 2010). In addition, PI3K activity has been linked to long-term potentiation (LTP) (Arendt et al., 2010; Man et al., 2003; Opazo et al., 2003; Sanna et al., 2002). Conversely, we have shown that the phosphatase activity of PTEN (phosphatase and tensin homolog deleted on chromosome ten), which antagonizes PI3K signaling by decreasing PIP_3 levels (Maehama and Dixon, 1999), depresses synaptic transmission and is specifically required for NMDA receptor (NMDAR)-dependent long-term depression (LTD) (Jurado et al., 2010). Therefore, upregulation of the PIP_3 pathway is generally associated with synaptic potentiation, whereas downregulation of the pathway is linked to synaptic depression (Knafo and Esteban, 2012; Peineau et al., 2007). However, this bidirectional correlation is far from clear. For example, a recent report suggests that PIP_3 levels actually decrease during LTP induction owing to a local redistribution (Ueda and Hayashi, 2013). Moreover, PI3K activity has also been linked to LTD (Kim et al., 2011). Therefore, the local dynamics of PIP_3 at synaptic compartments during plasticity are still unresolved.

One difficulty in studying the regulation of PIP_3 and its relation to synaptic function has been to visualize its compartmentalization and dynamics in living neurons. Overexpression of PIP_3-specific pleckstrin homology (PH) domains fused to GFP has been used to monitor changes in PIP_3 levels or distribution upon exogenous cell-wide activation of PI3K (Gray et al., 1999; Várnai et al., 2005), but they are not sensitive enough to detect basal PIP_3 levels or small local changes. The development of a PIP_3-specific PH domain tagged with a fluorescence resonance energy transfer (FRET) reporter has allowed real-time imaging of changes in PIP_3 levels in subcellular compartments (Aoki et al., 2005; Sato et al., 2003), including dendritic spines (Ueda and Hayashi, 2013). Using this reporter, together with biochemical experiments, we now show that PIP_3 undergoes a constant turnover at dendritic spines under basal conditions. Surprisingly, we found that both LTD and LTP trigger a similar increase in PIP_3 synthesis, which is dampened specifically during LTD because of the phosphatase activity of PTEN.

Journal of Cell Science (2014) 127, 5253–5260 doi:10.1242/jcs.156554

RESULTS

Detection of PIP_3 turnover under basal conditions

To investigate the basal distribution and dynamics of PIP_3 in living neurons, we used the fllip-pm reporter, an intramolecular FRET construct that undergoes FRET when bound to PIP_3 (Sato et al., 2003). We expressed fllip-pm in organotypic hippocampal slice cultures (see Materials and Methods) and carried out live confocal microscopy imaging experiments. Fllip-pm was expressed throughout CA1 pyramidal neurons (Fig. 1A), including the cell body, dendrites and dendritic spines (Fig. 1A,B). YFP and CFP fluorescence upon CFP excitation was quantified from spines and adjacent dendrites, and FRET efficiency was estimated as the YFP:CFP ratio after background subtraction (see representative examples in Fig. 1C). Average values of YFP:CFP ratios in dendritic spines are shown in Fig. 1D. To note, absolute acceptor:donor emission ratios (YFP:CFP) are not numerically equivalent to FRET efficiencies, because of the optical bleed-through between the channels. However, changes in FRET will be reflected in changes in YFP:CFP ratio, as is commonly used (Lam et al., 2012; Tsutsui et al., 2008). To confirm that the YFP:CFP ratio obtained under our optical conditions reflected a FRET reaction, we carried out similar experiments with a modified fllip-pm construct lacking the YFP FRET acceptor (ΔYFP). The YFP:CFP value obtained with ΔYFP was significantly lower than that obtained with fllip-pm (Fig. 1D, $P<0.0001$), indicating a net contribution of FRET to the YFP:CFP ratio obtained with fllip-pm.

We then evaluated the basal synthesis and turnover of PIP_3 in dendritic spines. To this end, we pharmacologically inhibited PTEN, the lipid phosphatase that converts $PI(3,4,5)P_3$ into phosphatidylinositol 4,5-bisphosphate [$PI(4,5)P_2$], with 15 nM bpV(HOpic) [dipotassium bisperoxo(5-hydroxypyridine-2-carboxyl)oxovanadate], a specific PTEN inhibitor (Schmid et al., 2004). As shown in Fig. 1D ('bpV'), PTEN inhibition produced a significant increase in FRET values in spines ($P<0.0001$; see a representative example in Fig. 1C). Conversely, inhibition of the PIP_3-synthesizing enzyme PI3K with 10 μM LY294002 (LY; a specific PI3K inhibitor Vanhaesebroeck et al., 2001) resulted in a significant decrease in FRET signal in the spine, as compared to the baseline value (Fig. 1D, $P=0.01$; see

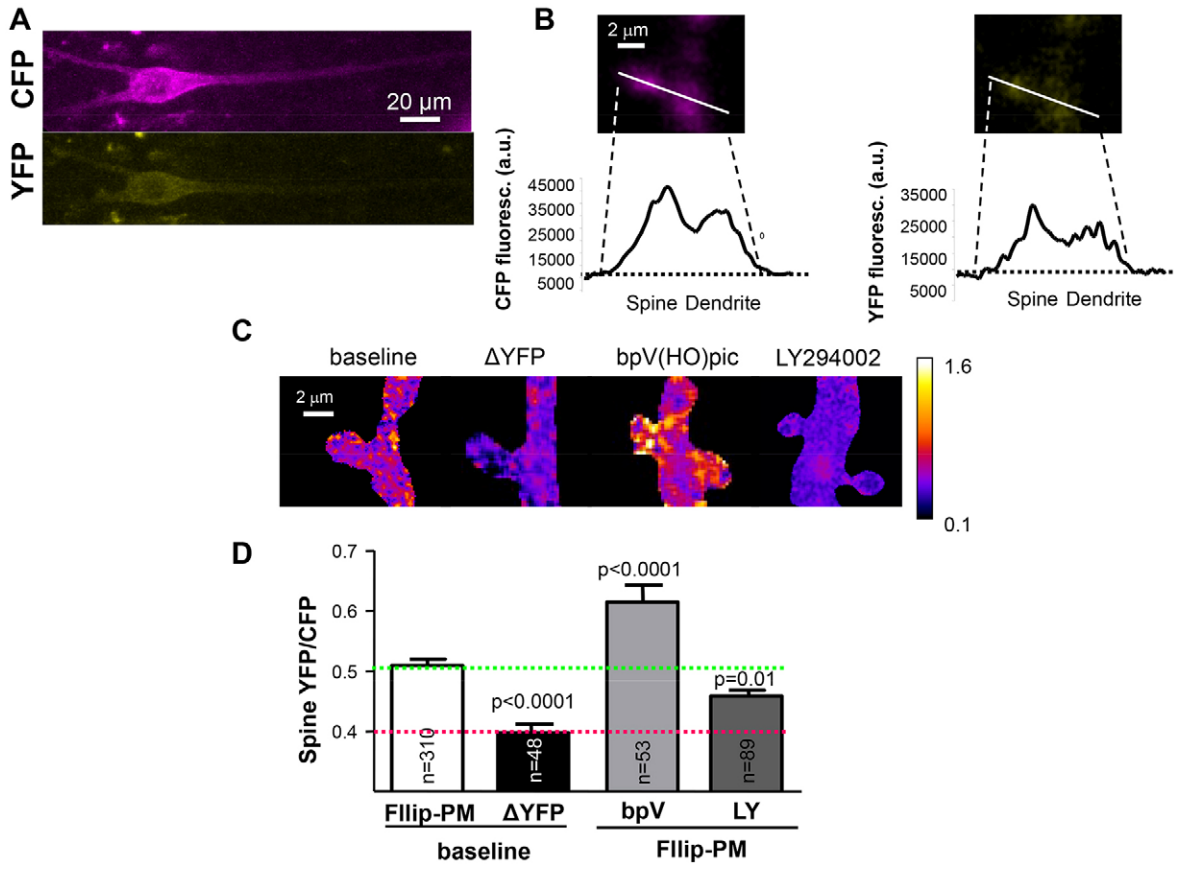

Fig. 1. PIP_3 levels in dendritic spines are detectable by FRET and undergo basal turnover. (A) Representative example of a CA1 pyramidal neuron expressing fllip-pm. Images of CFP and YFP fluorescence upon CFP excitation are shown. (B) Schematic of YFP and CFP fluorescence (fluoresc.) quantification at spines and dendritic shafts obtained from images taken using confocal microscopy. FRET signal is approximated as the ratio of YFP:CFP fluorescence after background subtractions. a.u., arbitrary units. (C) Example of FRET images calculated as pixel-by-pixel ratios from YFP and CFP fluorescence images. Fllip-pm-expressing neurons were left untreated (left-most image) or were treated with bpV(HOpic) (15 nM) or LY294002 (10 μM), as indicated, for 1 h before imaging. Second left-most image was obtained from a neuron expressing ΔYFP. These ratio images are shown for visualization purposes – comparisons of FRET values for statistical purposes were always carried out using integrated YFP and CFP intensities, from which the YFP:CFP ratio was then calculated. (D) Average spine and dendrite values of YFP:CFP ratios from slices expressing ΔYFP (black column) or fllip-pm without treatment (white column) or with 15 nM bpV(HOpic) (light gray) or 1-h treatment with 10 μM LY294002 (dark gray). For comparison across conditions, green and red lines show baseline YFP:CFP values for Fllip-PM and ΔYFP, respectively. *n*, number of spines. Data show the mean+s.e.m.; statistical significance was calculated according to the Mann–Whitney test.

Journal of Cell Science (2014) 127, 5253–5260 doi:10.1242/jcs.156554

representative spine in Fig. 1C). To note, this value cannot be lower than the YFP:CFP ratio with ΔYFP, which represents the lowest possible ratio in the absence of FRET (Fig. 1D, red line). These results confirm the interpretation that the fllip-pm FRET signal is indeed reporting PIP_3 levels in spines. In addition, these data indicate that basal PIP_3 in spines undergoes a constant metabolic turnover in resting (not stimulated) neurons, under the action of synthetic (PI3K) and degradative (PTEN) activities.

Transient increase in PIP_3 synthesis during LTD induction and modulation by PTEN

Induction of NMDAR-dependent LTD has been shown to inhibit the downstream PI3K effector Akt, and consequently to activate GSK3β (Peineau et al., 2007). In agreement with these biochemical observations, both PTEN (Jurado et al., 2010) and GSK3β (Peineau et al., 2007) are required for LTD. By contrast, a specific isoform of PI3K has been recently shown to be required for LTD (Kim et al., 2011). Therefore, we decided to directly monitor PIP_3 levels in dendritic spines during LTD. Induction of NMDAR-dependent LTD was carried out with a 5-min application of 20 µM NMDA – a protocol termed 'chemical LTD' (cLTD). This is a well-established protocol to induce a form of NMDAR-dependent LTD that electrophysiologically and biochemically mimics synaptically induced LTD (Fernández-Monreal et al., 2012; Lee et al., 1998) (supplementary material Fig. S1A). Example images of spines before (baseline), during (cLTD) and after (washout) cLTD induction are shown in Fig. 2A (upper panels). Quantification of YFP:CFP ratios from these images revealed no significant change in the spine or dendrite throughout the experiment (scatter plots of spine populations in Fig. 2C, left panels; average FRET values in spines and dendrites in Fig. 2D, gray columns). These results suggest that LTD induction proceeds without net changes in PIP_3 levels.

We have previously reported that the PIP_3 phosphatase PTEN is recruited to the postsynaptic membrane upon NMDAR activation during LTD induction, and is required for NMDAR-dependent LTD expression (Jurado et al., 2010). These results suggest that PTEN might participate in the modulation of PIP_3

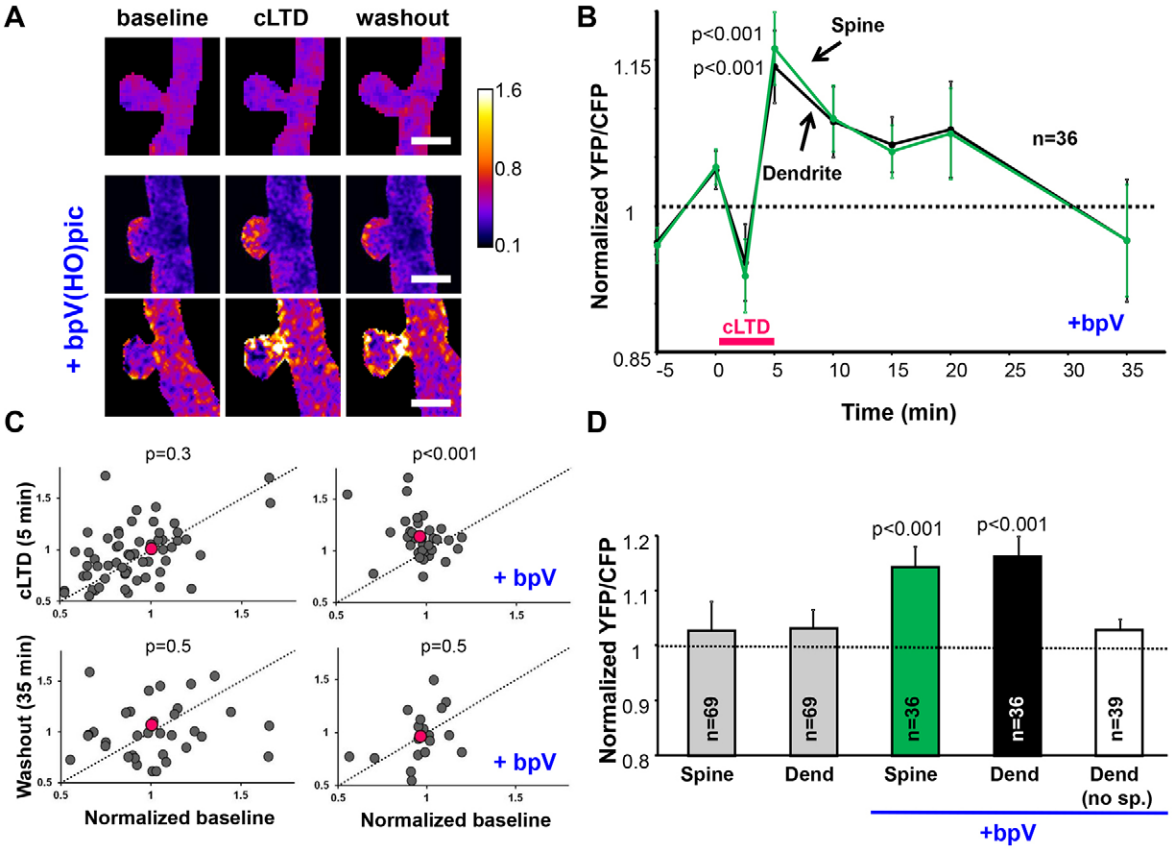

Fig. 2. Induction of LTD transiently increases PIP_3 levels in the presence of PTEN inhibitors. (A) FRET ratio images, calculated as described for Fig. 1B, of spines undergoing LTD induction in the absence (upper row) or presence (middle and lower rows) of the PTEN inhibitor bpV(HOpic). Scale bars: 2 µm. (B) Timecourse of changes in FRET (YFP:CFP) ratios in spines (green) and dendrites (black) during cLTD induction (magenta bar), in the presence of the PTEN inhibitor [15 nM bpV(HOpic)]. Values are normalized to the average baseline signal of each spine or dendrite. *n*, number of spine/dendrite pairs. Data show the mean±s.e.m.; *P*-values are calculated by pairwise comparisons of FRET ratios at 5 min with respect to the average baseline for each spine or dendrite (Wilcoxon test). (C) Population scatter plots of the same FRET ratios used in B, showing the values obtained from individual spines in the absence (left) or presence (right) of the PTEN inhibitor bpV(HOpic). The red datapoints correspond to the mean values from the population. Upper panels, FRET values after cLTD induction (5 min) versus the baseline FRET for each individual spine. Values are normalized to the average baseline. A leftward shift from the diagonal indicates a net increase in FRET. Lower panels, FRET values during the washout of cLTD (35 min) versus baseline values. *P*-values were calculated by pairwise comparisons with respect to the baseline for each spine (Wilcoxon test). (D) Summary of average FRET changes during LTD induction in spines (green), dendrites (dend, black) or dendritic regions away from spines (no sp., white) with PTEN inhibition. Corresponding values in the absence of the PTEN inhibitor are shown by the gray columns. *n*, number of spine/dendrite pairs. Data show the mean+s.e.m.; *P*-values were calculated as for B and C.

Journal of Cell Science (2014) 127, 5253–5260 doi:10.1242/jcs.156554

levels during LTD. To directly test this hypothesis, we repeated the cLTD imaging experiments with slices pretreated for 1 h with the specific PTEN inhibitor bpV(HOpic) (15 nM; the inhibitor was also present during LTD induction and washout). As shown in Fig. 2B, in the absence of PTEN activity, LTD induction led to a significant increase in PIP_3 levels in both spines and the adjacent dendritic shaft, with respect to baseline values (see representative examples in Fig. 2A, middle and lower panel rows). It should be noted that this increase occurs on top of the already elevated baseline levels generated upon PTEN inhibition (Fig. 1D). These changes were transient as PIP_3 levels gradually decayed to baseline values after the LTD induction (Fig. 2B). This increase in PIP_3 signal was detectable in most spines as demonstrated with population scatter plots (Fig. 2C, upper right panel), where FRET values are plotted for each individual spine, with the *x*-axis representing the YFP:CFP ratio at baseline and the *y*-axis representing the corresponding value at different time points during the LTD experiment. The population left-shift from the diagonal at 5 min cLTD indicates that most spines had increased FRET values with respect to their baseline at this time point. This left-shift is transient, as the population is equally scattered at both sides of the diagonal by the end of the washout following LTD induction (Fig. 2C, lower right panel). Interestingly, this increase in PIP_3 is associated with the spine. As shown in Fig. 2D (white column), there was no significant increase in PIP_3 signal in the dendritic shaft sampled away from spines (>2 µm). Taken together, these results indicate that induction of NMDAR-dependent LTD does not decrease PIP_3 levels. On the contrary, LTD induction has the potential to increase PIP_3 in the spines and the immediately adjacent dendritic shaft, but this increase is normally masked by the activity of PTEN.

Transient increase in PIP_3 levels during LTP induction

Another major form of NMDAR-dependent synaptic plasticity in the hippocampus is LTP. Several reports have suggested a role for PI3K in both the induction and expression of LTP (Arendt et al., 2010; Chen et al., 2005; Horwood et al., 2006; Man et al., 2003; Opazo et al., 2003; Sanna et al., 2002). However, it has been recently reported that LTP induction triggers a redistribution of PIP_3 within spines, without net synthesis or degradation (Ueda and Hayashi, 2013).

We have explored this issue by expressing fllip-pm in organotypic slice cultures and measuring PIP_3-induced FRET changes in spines and adjacent dendrites while inducing LTP using a pharmacological protocol (cLTP). This protocol drives global neuronal bursting, resulting in robust synaptic potentiation (Kopec et al., 2006; Otmakhov et al., 2004; supplementary material Fig. S1B). Images were taken before (baseline), during (cLTP) and after (washout) LTP induction. Fluorescence signals were analyzed as described above and FRET values were normalized to the average baseline values for each spine and dendrite. Example images of the change in FRET signals of spines undergoing cLTP are shown in Fig. 3A.

As shown in Fig. 3B, LTP induction produced a small but significant increase in PIP_3 signal in dendritic spines ($P<0.001$) and adjacent dendritic shafts ($P=0.02$), which gradually decayed to baseline values shortly after induction (Fig. 3B). In contrast to LTD, PTEN inhibition did not significantly alter the extent or duration of PIP_3 accumulation in response to LTP induction (Fig. 3B, blue; shown only for spines, for simplicity). Population scatter plots indicate that the increase in PIP_3 was a generalized effect across most spines (leftward shift from the diagonal in Fig. 3C, upper left panel) and was transient (equivalent scatter across the diagonal in Fig. 3C, lower left panel). Again, a similar behavior was observed in the presence of the PTEN inhibitor (Fig. 3C, right panels). The increase in PIP_3 was still localized to the vicinity of dendritic spines, as dendritic regions away from the base of spines (>2 µm) did not display a significant change in PIP_3 during LTP induction (Fig. 3D, white column).

Importantly, this increase in PIP_3 signal was dependent on NMDAR activation and PI3K activity, as demonstrated by the blockade of the YFP:CFP increase when LTP was induced in the presence of either the NMDAR antagonist APV (DL-2-amino-5-phosphonopentanoic acid, 0.1 mM) or the PI3K inhibitor LY294002 (10 µM) (Fig. 3D, gray columns). These inhibitors were present in the perfusion solution during baseline, LTP induction and washout. These results indicate that the accumulation of PIP_3 upon NMDAR activation is due to net synthesis by PI3K and not to PIP_3 redistribution.

As a control, similar experiments carried out with ΔYFP did not show changes in YFP:CFP ratio (Fig. 3D, purple columns), indicating that the observed increase with fllip-pm is not due to changes in CFP optical bleed-through. Additionally, we also monitored potential changes in intrinsic YFP fluorescence by directly exciting the YFP fluorophore in fllip-pm with a different laser line (514 nm). As shown in Fig. 3E, no changes in YFP fluorescence were observed during cLTP experiments. These two important controls support our interpretation that the LTP-induced changes in YFP:CFP ratio are due to PIP_3-driven FRET and not to optical or spectral changes in CFP or YFP fluorescence.

Upregulation of the PIP_3 pathway during LTP induction

Our observation of increased PIP_3 levels upon LTP induction contrasts with previously published results (Ueda and Hayashi, 2013). Therefore, we decided to validate these data with an independent biochemical approach. To this end, we performed enzyme-linked immunosorbent assay (ELISA) quantifications of PIP_3 on synaptosomal extracts from organotypic slices during cLTP experiments. Owing to the sensitivity of the technique, a large number of slices (35–45) are required for each synaptosomal fractionation (see Materials and Methods). Therefore, an *n* value of 1 in this experiment represents the average of 35–45 slices. As shown in Fig. 4A, PIP_3 levels increased during cLTP induction and returned to basal levels after washout. This result supports the FRET data, indicating that PIP_3 levels transiently increase in dendritic spines (Fig. 3) and in synaptosomal extracts (Fig. 4A) during cLTP induction. In addition, this biochemical method reports absolute levels of PIP_3 (see legend for Fig. 4A). Therefore, the approximately twofold increase in PIP_3 observed with this assay more likely reflects the actual change in PIP_3 with LTP, which is then translated into a 10% change in FRET signal (Fig. 3B,D) under our optical conditions.

An increase in PIP_3 levels upon LTP induction would be expected to activate downstream effectors of this pathway, such as Akt. To verify this observation in our experimental system, we performed immunoblotting analysis with antibodies against phosphorylated Akt. As shown in Fig. 4B, phosphorylation of Akt at both Ser473 and Thr308 was significantly increased during cLTP induction. These data show that downstream effectors of the PIP_3 pathway are transiently activated during LTP induction.

Journal of Cell Science (2014) 127, 5253–5260 doi:10.1242/jcs.156554

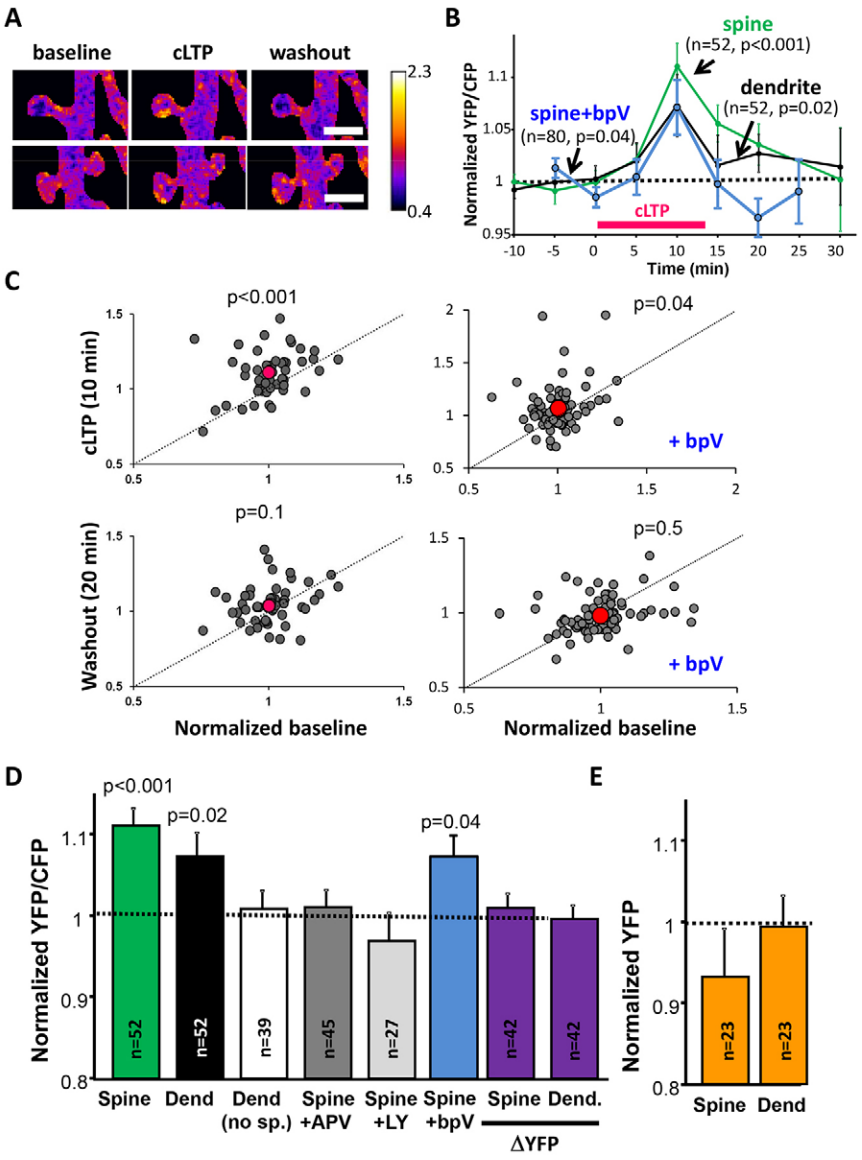

Fig. 3. Induction of LTP transiently increases PIP_3 levels. (A) Examples of YFP:CFP ratio images, calculated as described for Fig. 1C, to display changes in FRET ratios in spines undergoing LTP induction. Scale bars: 2 μm. (B) Timecourse of cLTP induction (magenta bar) showing changes in FRET (YFP:CFP) ratios in spines (green) and dendrites (black) in the absence of bpV(HOpic) or in spines in the presence of bpV(HOpic) (blue). Values are normalized to the average baseline signal of each spine or dendrite. *n*, number of spines and dendrites. Data show the mean±s.e.m.; *P*-values were calculated by pairwise comparisons of FRET ratios at 10 min with respect to the average baseline for each spine or dendrite (Wilcoxon test). (C) Population scatter plots of the same FRET ratios used in B, showing the values obtained from individual spines in the absence (left) or presence (right) of the PTEN inhibitor bpV(HOpic). The red datapoints correspond to the mean values from the population. Upper panels, FRET values at 10 min after the beginning of cLTP induction versus the baseline FRET for each individual spine. Values are normalized to the average baseline. Leftward shift from the diagonal indicates a net increase in FRET. Lower panels, FRET values during the washout of cLTP (20 min) versus baseline values. *P*-values are calculated by pairwise comparisons with respect to the baseline for each spine (Wilcoxon test). (D) Summary of average FRET ratios obtained 10 min after the beginning of cLTP induction. Values are plotted for spines (green), adjacent dendrites (dend, black) and dendritic regions away from spines (no sp., white). A similar analysis was carried out with slices incubated throughout the course of the experiment with 20 μM APV (dark gray), 10 μM LY294002 (light gray) or 15 nM bpV(HOpic) (blue) and with slices expressing the ΔYFP probe (purple). Values are normalized to the average baseline of each spine or dendrite under the different conditions. *n*, number of spine/dendrite pairs. Data show the mean+s.e.m.; *P*-values were calculated as for B, C. (E) Normalized YFP fluorescence values obtained with fllip-pm 10 min after the beginning of cLTP induction, by directly exciting YFP with a 514-nm laser line. Values are normalized to their respective baselines and plotted for spines and adjacent dendrites. *n*, number of spine/dendrite pairs. Data show the mean+s.e.m.

It is important to keep in mind that synaptosomal extracts are expected to contain both pre- and postsynaptic elements. In addition, synaptosomal fractionations do not yield pure synaptic compartments and, therefore, some degree of extrasynaptic membrane is also likely to be present in these preparations. Nevertheless, taken together, these data strengthen our interpretation that LTP induction is accompanied by a rapid upregulation of PIP_3 levels at synaptic compartments and activation of downstream signaling effectors.

DISCUSSION

In this study we have reported, for the first time, that PIP_3 is transiently upregulated at dendritic spines during synaptic plasticity induction upon NMDAR activation. It should be noted that this effect is likely due to the activation of PI3K and not to a transient inhibition of PTEN or redistribution of PIP_3 within the cell, because these changes are observed in the presence of PTEN inhibitors and are blocked by inhibitors of PI3K activity. Interestingly, in the case of NMDAR-dependent LTD, the potential increase in PIP_3 is specifically quenched by the activity of PTEN.

Concerning LTP, our results contrast with a recent publication where PIP_3 concentration was found to decrease upon induction of LTP (Ueda and Hayashi, 2013). The authors concluded that this decrease was not due to PIP_3 degradation but, rather, was due to a non-enzymatic dilution of PIP_3 upon spine enlargement during structural plasticity. Our pharmacological protocol for LTP induction produces a more modest increase in spine size than the glutamate uncaging protocol used in the previous study (Ueda and Hayashi, 2013). Therefore, it is possible that we were able to detect a net increase in PIP_3 levels owing to a lesser volume dilution in our system. In addition, using synaptosomal fractionations and biochemical detection, we confirmed the increase in PIP_3 levels and the activation of downstream effectors of this pathway (Akt phosphorylation) upon LTP induction.

What are the mechanisms by which both LTP and LTD induction would trigger PI3K activation? It has been shown that activation of NMDARs during LTP leads to the activation of Ras (Harvey et al., 2008) and downstream signaling cascades (Kim et al., 2003; Komiyama et al., 2002; Li et al., 2006; Schmitt et al., 2005; Zhu et al., 2002). In turn, Ras can activate PI3K by direct

Journal of Cell Science (2014) 127, 5253–5260 doi:10.1242/jcs.156554

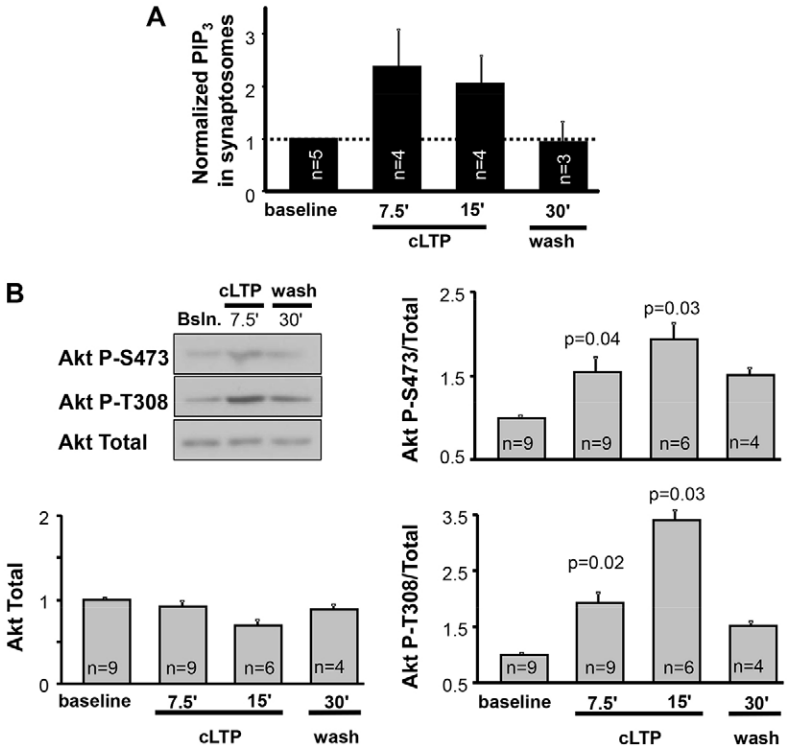

Fig. 4. Induction of LTP transiently activates the PI3K pathway. (A) Synaptosomes were prepared from untreated organotypic slices (baseline) or from slices undergoing cLTP (7.5 and 15-min induction, and 30 min of washout after induction). A total of 1 mg of protein was used in each case for synaptosomal preparations. PIP_3 levels were quantified from synaptosomes using the Mass ELISA Kit from Echelon. PIP_3 values were normalized to untreated (baseline) slices. This value corresponded to 0.43±0.17 pmol (mean±s.e.m.; the detection limit for PIP_3 is 0.04 pmol, according to the manufacturers). Data show the mean+s.e.m. (B) Quantification of phosphorylated Akt (Ser473 and Thr308) and total Akt expression from slices undergoing cLTP, normalized to their respective baseline (Bsln., untreated slices). *n*, number of experiments for each point. *P*-values were determined by comparing cLTP versus baseline (Wilcoxon test). Representative western blots are shown.

interaction with the p110 catalytic subunit of class I PI3Ks, leading to the activation of its lipid kinase activity and synthesis of PIP_3 (Suire et al., 2002). Downstream effectors of PIP_3 would lead to the activation of Akt and ERK pathways (Knafo and Esteban, 2012; Perkinton et al., 2002; Sutton and Chandler, 2002; Sweatt, 2004). Growing evidence indicates that key elements of this pathway are localized in dendritic spines (Majumdar et al., 2011; Man et al., 2003; Peineau et al., 2007), supporting the notion that both PIP_3 synthesis and downstream signaling might be highly compartmentalized for the local control of postsynaptic function during plasticity.

Does this scenario apply to LTD? Interestingly, two distinct Ca^{2+}-dependent Ras activators, RASGRF1 and RASGRF2, have been implicated in LTP and LTD, respectively, by coupling to different MAPK pathways (Li et al., 2006). However, it has also been reported that Ras activity is not required for LTD (Zhu et al., 2002). PI3Ks are a complex family of catalytic and regulatory subunits, which can integrate a variety of upstream signaling events (Vanhaesebroeck et al., 2010). Alternative 'classical' PI3K activators are G-protein-coupled receptors (GPCRs). Indeed, NMDAR-dependent LTD in the visual cortex has been shown to require concurrent activation of several GPCRs (Choi et al., 2005), which might also modulate the balance between LTP and LTD (Huang et al., 2012). Moreover, a specific isoform of PI3K, p110γ, is required for NMDAR-dependent LTD (Kim et al., 2011), and this isoform can be activated by Gβγ subunits *in vitro* (Maier et al., 1999). In addition, Rab5, an endocytic factor that is activated during LTD (Brown et al., 2005), has been found to interact with catalytic and regulatory subunits of PI3K (Christoforidis et al., 1999). Activation of the PI3K pathway might also be mediated by the small GTPase Rap1a (Tsygankova et al., 2001), which is also an effector of AMPAR internalization during LTD (Zhu et al., 2002). Therefore, it is premature to propose a precise effector linking LTD and PI3K. Nevertheless, our data provide two important pieces of new information. First, that downstream of LTP and LTD induction, there is a point of convergence at the level of PI3K activation, and second, that this convergence is subsequently resolved by the specific engagement of PTEN during LTD, which prevents PIP_3 accumulation. We have recently reported that PTEN is recruited to the postsynaptic membrane upon LTD induction (Jurado et al., 2010). It remains to be discovered what determines the specific engagement of PTEN during LTD (and not during LTP), but this appears to be a crucial mechanism by which similar upstream events (NMDAR opening and PI3K activation) are relayed into divergent synaptic outcomes (potentiation or depression). Indeed, shunting PIP_3 might be important to ensure LTD expression, given that GSK3β is required for LTD and this kinase would otherwise be inhibited by the activation of the PIP_3 pathway through Akt phosphorylation (Peineau et al., 2007).

And finally, does this mean that the role of PTEN during LTD is just to prevent a 'collateral' increase in PIP_3 downstream of NMDAR activation? PTEN is itself a complicated signaling hub, with lipid and protein phosphatase activities, as well as phosphatase-independent functions (Song et al., 2012). Therefore, it is not unreasonable that PTEN will have additional roles in LTD besides preventing a potentially counterproductive PIP_3 accumulation. Nevertheless, we should keep in mind that most of the effectors in these pathways are highly pleiotropic (for example, Ras couples to PI3K and MAPK pathways, with further branching in downstream signaling). Therefore, it is interesting to speculate that for some forms of synaptic plasticity, such as LTD, pathway specificity might be achieved by shutting down (or quenching) specific downstream cascades, while leaving other avenues open. In conclusion, we have reported here that PIP_3 is tightly regulated in dendritic spines during synaptic plasticity events, where specific combinations of PI3K and PTEN activities determine the synaptic outcome after plasticity induction.

Journal of Cell Science (2014) 127, 5253–5260 doi:10.1242/jcs.156554

MATERIALS AND METHODS

Ethics statement

All biosafety procedures and animal care protocols were approved by the bioethics committee from the Consejo Superior de Investigaciones Cientificas (CSIC) and were carried out according to the guidelines set out in the European Community Council Directives (2010/63UE: Council Decision of 22 September 2010).

Expression of recombinant proteins

The fllip-pm construct was generously provided by Yoshio Umezawa (University of Tokyo, Japan). ΔYFP was derived by removing part of the PH domain and YFP from the original fllip-pm. These constructs were recloned into pSinRep5 for expression using Sindbis virus (Schlesinger and Dubensky, 1999). Recombinant proteins were expressed in organotypic hippocampal slice cultures (Gerges et al., 2005). Briefly, hippocampal slices were prepared from young rats (postnatal days 5–7) and placed in culture on semiporous membranes. After 4–5 days in culture, the recombinant gene was delivered into the slice using Sindbis virus. This method led to robust expression of the recombinant proteins after 16–24 h, when imaging experiments were carried out.

Antibodies

Antibodies used were against total Akt (Cell Signaling Technology, catalog number 8272; RRID, AB_329827), phospho-Thr308 Akt (Cell Signaling Technology, catalog number 4056; RRID, AB_331163) and phospho-Ser473 Akt (Cell Signaling Technology, catalog number 4060; RRID, AB_916024).

Fluorescence resonance energy transfer

Fluorescence images were collected by confocal microscopy using a 405-nm Blue Diode laser as the light source for excitation. CFP and YFP fluorescence emission were collected on separate photomultipliers using band-pass filters. The sensitivity of the photomultipliers was constant throughout all experiments to allow comparison of YFP:CFP ratios across different experiments. Laser power was varied to compensate for variability in expression levels of the construct. Digital images were analyzed using NIH ImageJ or Zeiss Zen software. FRET efficiency was then estimated as the ratio of YFP:CFP fluorescence. Under this optical configuration, a fraction of the CFP signal 'leaked' into the YFP channel (as evidenced with the ΔYFP construct, Fig. 1). This implies that the YFP:CFP ratio would be larger than zero even in the absence of FRET. This signal bleed-through was purely optical and constant irrespective of FRET conditions. Therefore, we did not attempt to correct for it.

Pharmacological treatments during live imaging

Imaging experiments were performed on organotypic slice cultures at 5–10 days *in vitro* after expression of the recombinant protein for 24 h. Images of dendritic branches and spines were taken using the optical settings described above. For acute manipulations of PIP_3 levels, slices were exposed to either the PI3K inhibitor LY294002 (10 µM) or to the PTEN inhibitor bpV(HOpic) (15 nM) for 1–2 h prior to imaging.

For synaptic plasticity experiments, baseline images were obtained over a timecourse of 5–10 min while the slices were perfused at 30℃ with artificial cerebrospinal fluid (ACSF) containing 119 mM NaCl, 2.5 mM KCl, 4 mM $CaCl_2$, 4 mM $MgCl_2$, 26 mM $NaHCO_3$, 1 mM NaH_2PO_4, 11 mM glucose, 50 µM picrotoxin and 6 µM 2-chloroadenosine. For cLTP induction (Otmakhov et al., 2004), perfusion solution was exchanged with a modified ACSF lacking $MgCl_2$ and 2-chloroadenosine and adding 0.1 µM rolipram and 50 µM forskolin. Slices were perfused with cLTP ACSF for 15 min and then returned to regular ACSF for the remainder of the timecourse (washout). For cLTD induction, slices were perfused with ACSF plus 20 µM NMDA for 5 min, before returning to regular ACSF (washout). Some experiments were carried out using 0.1 mM APV (NMDAR antagonist), 10 µM LY294002 (PI3K inhibitor) or 15 nM bpV(HOpic) (PTEN inhibitor) in the perfusion solutions. These inhibitors were pre-incubated with the slices for 30 min before the imaging session, and they were then present in the ACSF during baseline, synaptic plasticity induction and washout.

Electrophysiology

The recording chamber was perfused with ACSF, as described for live-imaging experiments. Electrophysiological recordings were obtained from CA1 pyramidal neurons. Synaptic responses were evoked with bipolar electrodes using single-voltage pulses (200 µs, up to 25 V). The stimulating electrodes were placed over Schaffer collateral fibers between 300 and 500 µm from the recorded cells. Data acquisition was carried out with Multiclamp 700A amplifiers and pClamp software (Molecular Devices). For whole-cell excitatory postsynaptic currents (EPSCs), (supplementary material Fig. S1A) patch-recording pipettes (3–6 MΩ) were filled with 115 mM cesium methanesulphonate, 20 mM CsCl, 10 mM HEPES, 2.5 mM $MgCl_2$, 4 mM disodium ATP, 0.4 mM trisodium GTP, 10 mM sodium phosphocreatine and 0.6 mM EGTA pH 7.25. For field excitatory postsynaptic potentials (fEPSPs) (supplementary material Fig. S1B), recording pipettes (0.8–0.2 MΩ) were filled with ACSF and placed in the stratum radiatum of the CA1 area.

ELISA PIP_3 quantification

Biochemical isolation of crude synaptosomes was carried out essentially as described previously (Carlin et al., 1980). Briefly, organotypic slices (between 35 and 45 slices per time point) were treated for cLTP induction as described above and were then homogenized in a Dounce glass homogenizer with a buffer containing 0.32 M sucrose, 1 mM $MgCl_2$, 0.5 mM $CaCl_2$, 10 mM HEPES, 1 mM EGTA, 1 mM dithiothreitol and a cocktail of protease inhibitors from Roche (Complete Mini EDTA-free). Proteins from this homogenate were quantified by using the Bradford assay and the same quantity of protein (around 1 mg) for the different conditions was spun down at 1400 ***g*** for 10 min at 4℃. The supernatant was kept and the pellet was resuspended in the same homogenization buffer and spun again at 710 ***g*** for 10 min at 4℃. Both supernatants were mixed and spun down at 11,600 ***g*** for 12 min at 4℃. The pellet (crude synaptosomal fraction) was resuspended in cold 8% trichloroacetic acid and centrifuged at 1500 ***g*** for 5 min. The pellet was then washed with a solution of 5% trichloroacetic acid and 1 mM EDTA, vortexed to resuspend and centrifuged again (215 ***g***, 5 min). To remove neutral lipids, we added 1 ml of methanol:$CHCl_3$ (2:1), vortexed at room temperature and centrifuged at 215 ***g*** for 5 min. The supernatant was discarded and acidic lipids were then extracted from the pellet by resuspending in 1 ml of methanol:$CHCl_3$:12 M HCl (80:40:1), vortexing at room temperature and centrifuging (215 ***g***, 5 min). The supernatant was then mixed with 333 µl of $CHCl_3$ and 666 µl of 0.1 M HCl, vortexed and centrifuged at 215 ***g*** for 5 min. The organic (lower) phase was collected and dried in a clean vial using a vacuum dryer. Dried lipids were used for PIP_3 quantification using the Mass ELISA Kit K-2500 (Echelon) according to the manufacturer's instructions.

Acknowledgements

We thank the personnel at the fluorescence microscopy facility of the CBMSO (SMOC) for their expert technical assistance, and members of the Esteban laboratory for their critical reading of the manuscript. We also thank Yoshio Umezawa (University of Tokyo, Japan) for his generous gift of the Fllip-pm construct.

Competing interests

The authors declare no competing interests.

Author contributions

K.L.A. and M.B. carried out most of the experimental work. A.L. performed the electrophysiology experiments and J.E.D. carried out some of the imaging experiments. M.M. prepared some of the reagents. K.L.A., M.B. and J.A.E. designed research, analyzed data and wrote the paper.

Funding

This work was supported by grants from the Spanish Ministry [grant numbers CSD-2010-00045 and SAF-2011-24730]; and Fundación Ramón Areces to J.A.E. M.B. is the recipient of a postdoctoral contract from the Instituto de Salud Carlos III; and a research award from the Fondation Bettencourt-Schuller (France).

Supplementary material

Supplementary material available online at
http://jcs.biologists.org/lookup/suppl/doi:10.1242/jcs.156554/-/DC1

References

Aoki, K., Nakamura, T., Fujikawa, K. and Matsuda, M. (2005). Local phosphatidylinositol 3,4,5-trisphosphate accumulation recruits Vav2 and Vav3 to activate Rac1/Cdc42 and initiate neurite outgrowth in nerve growth factor-stimulated PC12 cells. *Mol. Biol. Cell* **16**, 2207-2217.

Arendt, K. L., Royo, M., Fernández-Monreal, M., Knafo, S., Petrok, C. N., Martens, J. R. and Esteban, J. A. (2010). PIP3 controls synaptic function by maintaining AMPA receptor clustering at the postsynaptic membrane. *Nat. Neurosci.* **13**, 36-44.

Brown, T. C., Tran, I. C., Backos, D. S. and Esteban, J. A. (2005). NMDA receptor-dependent activation of the small GTPase Rab5 drives the removal of synaptic AMPA receptors during hippocampal LTD. *Neuron* **45**, 81-94.

Carlin, R. K., Grab, D. J., Cohen, R. S. and Siekevitz, P. (1980). Isolation and characterization of postsynaptic densities from various brain regions: enrichment of different types of postsynaptic densities. *J. Cell Biol.* **86**, 831-845.

Carlton, J. G. and Cullen, P. J. (2005). Coincidence detection in phosphoinositide signaling. *Trends Cell Biol.* **15**, 540-547.

Chen, X., Garelick, M. G., Wang, H., Lil, V., Athos, J. and Storm, D. R. (2005). PI3 kinase signaling is required for retrieval and extinction of contextual memory. *Nat. Neurosci.* **8**, 925-931.

Choi, S. Y., Chang, J., Jiang, B., Seol, G. H., Min, S. S., Han, J. S., Shin, H. S., Gallagher, M. and Kirkwood, A. (2005). Multiple receptors coupled to phospholipase C gate long-term depression in visual cortex. *J. Neurosci.* **25**, 11433-11443.

Christoforidis, S., Miaczynska, M., Ashman, K., Wilm, M., Zhao, L., Yip, S. C., Waterfield, M. D., Backer, J. M. and Zerial, M. (1999). Phosphatidylinositol-3-OH kinases are Rab5 effectors. *Nat. Cell Biol.* **1**, 249-252.

Czech, M. P. (2003). Dynamics of phosphoinositides in membrane retrieval and insertion. *Annu. Rev. Physiol.* **65**, 791-815.

Di Paolo, G. and De Camilli, P. (2006). Phosphoinositides in cell regulation and membrane dynamics. *Nature* **443**, 651-657.

Downes, C. P., Gray, A. and Lucocq, J. M. (2005). Probing phosphoinositide functions in signaling and membrane trafficking. *Trends Cell Biol.* **15**, 259-268.

Fernández-Monreal, M., Brown, T. C., Royo, M. and Esteban, J. A. (2012). The balance between receptor recycling and trafficking toward lysosomes determines synaptic strength during long-term depression. *J. Neurosci.* **32**, 13200-13205.

Gerges, N. Z., Brown, T. C., Correia, S. S. and Esteban, J. A. (2005). Analysis of Rab protein function in neurotransmitter receptor trafficking at hippocampal synapses. *Methods Enzymol.* **403**, 153-166.

Gray, A., Van Der Kaay, J. and Downes, C. P. (1999). The pleckstrin homology domains of protein kinase B and GRP1 (general receptor for phosphoinositides-1) are sensitive and selective probes for the cellular detection of phosphatidylinositol 3,4-bisphosphate and/or phosphatidylinositol 3,4,5-trisphosphate in vivo. *Biochem. J.* **344**, 929-936.

Harvey, C. D., Yasuda, R., Zhong, H. and Svoboda, K. (2008). The spread of Ras activity triggered by activation of a single dendritic spine. *Science* **321**, 136-140.

Horwood, J. M., Dufour, F., Laroche, S. and Davis, S. (2006). Signalling mechanisms mediated by the phosphoinositide 3-kinase/Akt cascade in synaptic plasticity and memory in the rat. *Eur. J. Neurosci.* **23**, 3375-3384.

Huang, S., Treviño, M., He, K., Ardiles, A., Pasquale, R., Guo, Y., Palacios, A., Huganir, R. and Kirkwood, A. (2012). Pull-push neuromodulation of LTP and LTD enables bidirectional experience-induced synaptic scaling in visual cortex. *Neuron* **73**, 497-510.

Jurado, S., Benoist, M., Lario, A., Knafo, S., Petrok, C. N. and Esteban, J. A. (2010). PTEN is recruited to the postsynaptic terminal for NMDA receptor-dependent long-term depression. *EMBO J.* **29**, 2827-2840.

Kim, J. H., Lee, H. K., Takamiya, K. and Huganir, R. L. (2003). The role of synaptic GTPase-activating protein in neuronal development and synaptic plasticity. *J. Neurosci.* **23**, 1119-1124.

Kim, J. I., Lee, H. R., Sim, S. E., Baek, J., Yu, N. K., Choi, J. H., Ko, H. G., Lee, Y. S., Park, S. W., Kwak, C. et al. (2011). PI3Kγ is required for NMDA receptor-dependent long-term depression and behavioral flexibility. *Nat. Neurosci.* **14**, 1447-1454.

Knafo, S. and Esteban, J. A. (2012). Common pathways for growth and for plasticity. *Curr. Opin. Neurobiol.* **22**, 405-411.

Komiyama, N. H., Watabe, A. M., Carlisle, H. J., Porter, K., Charlesworth, P., Monti, J., Strathdee, D. J., O'Carroll, C. M., Martin, S. J., Morris, R. G. et al. (2002). SynGAP regulates ERK/MAPK signaling, synaptic plasticity, and learning in the complex with postsynaptic density 95 and NMDA receptor. *J. Neurosci.* **22**, 9721-9732.

Kopec, C. D., Li, B., Wei, W., Boehm, J. and Malinow, R. (2006). Glutamate receptor exocytosis and spine enlargement during chemically induced long-term potentiation. *J. Neurosci.* **26**, 2000-2009.

Lam, A. J., St-Pierre, F., Gong, Y., Marshall, J. D., Cranfill, P. J., Baird, M. A., McKeown, M. R., Wiedenmann, J., Davidson, M. W., Schnitzer, M. J. et al. (2012). Improving FRET dynamic range with bright green and red fluorescent proteins. *Nat. Methods* **9**, 1005-1012.

Lee, H. K., Kameyama, K., Huganir, R. L. and Bear, M. F. (1998). NMDA induces long-term synaptic depression and dephosphorylation of the GluR1 subunit of AMPA receptors in hippocampus. *Neuron* **21**, 1151-1162.

Li, S., Tian, X., Hartley, D. M. and Feig, L. A. (2006). Distinct roles for Ras-guanine nucleotide-releasing factor 1 (Ras-GRF1) and Ras-GRF2 in the induction of long-term potentiation and long-term depression. *J. Neurosci.* **26**, 1721-1729.

Maehama, T. and Dixon, J. E. (1999). PTEN: a tumour suppressor that functions as a phospholipid phosphatase. *Trends Cell Biol.* **9**, 125-128.

Maier, U., Babich, A. and Nürnberg, B. (1999). Roles of non-catalytic subunits in gbetagamma-induced activation of class I phosphoinositide 3-kinase isoforms beta and gamma. *J. Biol. Chem.* **274**, 29311-29317.

Majumdar, D., Nebhan, C. A., Hu, L., Anderson, B. and Webb, D. J. (2011). An APPL1/Akt signaling complex regulates dendritic spine and synapse formation in hippocampal neurons. *Mol. Cell. Neurosci.* **46**, 633-644.

Man, H. Y., Wang, Q., Lu, W. Y., Ju, W., Ahmadian, G., Liu, L., D'Souza, S., Wong, T. P., Taghibiglou, C., Lu, J. et al. (2003). Activation of PI3-kinase is required for AMPA receptor insertion during LTP of mEPSCs in cultured hippocampal neurons. *Neuron* **38**, 611-624.

Ménager, C., Arimura, N., Fukata, Y. and Kaibuchi, K. (2004). PIP3 is involved in neuronal polarization and axon formation. *J. Neurochem.* **89**, 109-118.

Opazo, P., Watabe, A. M., Grant, S. G. and O'Dell, T. J. (2003). Phosphatidylinositol 3-kinase regulates the induction of long-term potentiation through extracellular signal-related kinase-independent mechanisms. *J. Neurosci.* **23**, 3679-3688.

Otmakhov, N., Khibnik, L., Otmakhova, N., Carpenter, S., Riahi, S., Asrican, B. and Lisman, J. (2004). Forskolin-induced LTP in the CA1 hippocampal region is NMDA receptor dependent. *J. Neurophysiol.* **91**, 1955-1962.

Peineau, S., Taghibiglou, C., Bradley, C., Wong, T. P., Liu, L., Lu, J., Lo, E., Wu, D., Saule, E., Bouschet, T. et al. (2007). LTP inhibits LTD in the hippocampus via regulation of GSK3beta. *Neuron* **53**, 703-717.

Perkinton, M. S., Ip, J. K., Wood, G. L., Crossthwaite, A. J. and Williams, R. J. (2002). Phosphatidylinositol 3-kinase is a central mediator of NMDA receptor signalling to MAP kinase (Erk1/2), Akt/PKB and CREB in striatal neurones. *J. Neurochem.* **80**, 239-254.

Sanna, P. P., Cammalleri, M., Berton, F., Simpson, C., Lutjens, R., Bloom, F. E. and Francesconi, W. (2002). Phosphatidylinositol 3-kinase is required for the expression but not for the induction or the maintenance of long-term potentiation in the hippocampal CA1 region. *J. Neurosci.* **22**, 3359-3365.

Sato, M., Ueda, Y., Takagi, T. and Umezawa, Y. (2003). Production of PtdInsP3 at endomembranes is triggered by receptor endocytosis. *Nat. Cell Biol.* **5**, 1016-1022.

Schlesinger, S. and Dubensky, T. W. (1999). Alphavirus vectors for gene expression and vaccines. *Curr. Opin. Biotechnol.* **10**, 434-439.

Schmid, A. C., Byrne, R. D., Vilar, R. and Woscholski, R. (2004). Bisperoxovanadium compounds are potent PTEN inhibitors. *FEBS Lett.* **566**, 35-38.

Schmitt, J. M., Guire, E. S., Saneyoshi, T. and Soderling, T. R. (2005). Calmodulin-dependent kinase kinase/calmodulin kinase I activity gates extracellular-regulated kinase-dependent long-term potentiation. *J. Neurosci.* **25**, 1281-1290.

Song, M. S., Salmena, L. and Pandolfi, P. P. (2012). The functions and regulation of the PTEN tumour suppressor. *Nat. Rev. Mol. Cell Biol.* **13**, 283-296.

Suire, S., Hawkins, P. and Stephens, L. (2002). Activation of phosphoinositide 3-kinase gamma by Ras. *Curr. Biol.* **12**, 1068-1075.

Sutton, G. and Chandler, L. J. (2002). Activity-dependent NMDA receptor-mediated activation of protein kinase B/Akt in cortical neuronal cultures. *J. Neurochem.* **82**, 1097-1105.

Sweatt, J. D. (2004). Mitogen-activated protein kinases in synaptic plasticity and memory. *Curr. Opin. Neurobiol.* **14**, 311-317.

Tsutsui, H., Karasawa, S., Okamura, Y. and Miyawaki, A. (2008). Improving membrane voltage measurements using FRET with new fluorescent proteins. *Nat. Methods* **5**, 683-685.

Tsygankova, O. M., Saavedra, A., Rebhun, J. F., Quilliam, L. A. and Meinkoth, J. L. (2001). Coordinated regulation of Rap1 and thyroid differentiation by cyclic AMP and protein kinase A. *Mol. Cell. Biol.* **21**, 1921-1929.

Ueda, Y. and Hayashi, Y. (2013). PIP_3 regulates spinule formation in dendritic spines during structural long-term potentiation. *J. Neurosci.* **33**, 11040-11047.

Vanhaesebroeck, B., Leevers, S. J., Ahmadi, K., Timms, J., Katso, R., Driscoll, P. C., Woscholski, R., Parker, P. J. and Waterfield, M. D. (2001). Synthesis and function of 3-phosphorylated inositol lipids. *Annu. Rev. Biochem.* **70**, 535-602.

Vanhaesebroeck, B., Guillermet-Guibert, J., Graupera, M. and Bilanges, B. (2010). The emerging mechanisms of isoform-specific PI3K signalling. *Nat. Rev. Mol. Cell Biol.* **11**, 329-341.

Várnai, P., Bondeva, T., Tamás, P., Tóth, B., Buday, L., Hunyady, L. and Balla, T. (2005). Selective cellular effects of overexpressed pleckstrin-homology domains that recognize PtdIns(3,4,5)P3 suggest their interaction with protein binding partners. *J. Cell Sci.* **118**, 4879-4888.

Wenk, M. R. and De Camilli, P. (2004). Protein-lipid interactions and phosphoinositide metabolism in membrane traffic: insights from vesicle recycling in nerve terminals. *Proc. Natl. Acad. Sci. USA* **101**, 8262-8269.

Zhu, J. J., Qin, Y., Zhao, M., Van Aelst, L. and Malinow, R. (2002). Ras and Rap control AMPA receptor trafficking during synaptic plasticity. *Cell* **110**, 443-455.